

Ultrastrongly-coupled and Directionally-nonreciprocal Magnon-polaritons in Magnetochiral Metamolecules

Kentaro Mita,¹ Takahiro Chiba,^{2,3} Toshiyuki Kodama,⁴ Tetsuya Ueda,⁵ Toshihiro Nakanishi,⁶ Kei Sawada,⁷ and Satoshi Tomita^{1,4,*}

¹*Department of Physics, Graduate School of Science, Tohoku University, Sendai 980-8578, Japan*

²*Frontier Research Institute for Interdisciplinary Sciences, Tohoku University, Sendai 980-8578, Japan*

³*Department of Applied Physics, Graduate School of Engineering, Tohoku University, Sendai 980-8579, Japan*

⁴*Institute for Excellence in Higher Education, Tohoku University, Sendai, 980-8576, Japan*

⁵*Department of Electrical Engineering and Electronics, Kyoto Institute of Technology, Kyoto 606-8585, Japan*

⁶*Department of Electronic Science and Engineering, Kyoto University, Kyoto 615-8510, Japan*

⁷*RIKEN SPring-8 Center, Sayo 679-5148, Japan*

(Dated: October 23, 2024)

We experimentally demonstrate magnon-polaritons with ultrastrong coupling and directional nonreciprocity in a metamolecule lacking time-reversal and space-inversion symmetries at room temperature. These experimental results are reproduced well via numerical simulations and theoretical consideration. Ultrastrong coupling is due to a direct interaction of magnons in the magnetic meta-atom with microwave photons confined in the chiral meta-atom as a resonator. Our results reveal a crucial step in identifying deepstrongly-coupled and optically-moving magnon-polaritons for hybrid quantum systems, synthetic gauge fields, and quasi-particle “chemistry” using metamaterials.

Introduction – Condensed matter physics is a field of various quasi-particles with elementary excitations. Integrating different quasi-particles has led to novel and intriguing properties of matters and opened an essential pathway toward frontiers in physics [1, 2]. A magnon, a quantized elementary excitation in magnets, can be transformed to magnon-polariton (MP) when it is coupled to alternating current (AC) electromagnetic fields, namely photons. The MP has gained attention particularly in quantum information technology and spintronics [3, 4] for applications to hybrid quantum systems [5].

Magnons and photons are coherently coupled – strong coupling – if the coupling constant, g is larger than the dissipation rate, κ , in a resonator and oscillator ($g > \kappa$), generating MP. Here, g is given by $g = (\omega_+ - \omega_-)/2$, where ω_{\pm} is the hybridized eigenmodes at the crossing point of the original modes. Such coherent coupling of magnons with photons having a frequency of $\omega/2\pi$ gives rise to the dispersion anti-crossing due to the hybridization. The anti-crossing is evaluated using Rabi-like level repulsion of $2g/2\pi$, which is proportional to a coupling ratio of g/ω . While the strong coupling is characterized by $g > \kappa$, an ultrastrong magnon-photon coupling is represented by $g > \kappa$ and $g/\omega > 0.1$, which is indispensable toward the quantum regime [6]. The ultrastrongly-coupled MPs have been demonstrated at microwave frequencies using magnetic heterostructures composed of superconductors [7–9]. They are, however, operated at cryogenic temperatures. Therefore, operating the ultrastrongly-coupled MPs at room temperature remains challenging.

The ultrastrongly-coupled MP is inherently nonreciprocal owing to the breaking of time-reversal symmetry by magnetization or magnetic fields [10]. With the additional breaking of the space-inversion symme-

try, the nonreciprocity results in a transmission amplitude (and phase) difference depending on the propagation direction of photons. However, such a directionally-nonreciprocal optical phenomenon has yet to be observed in ultrastrongly-coupled systems, except for dissipative [11] or strong [12] magnon-photon coupling. The directionally-nonreciprocal phenomena exist in natural chiral molecules [13–15], multiferroic materials [16], and metamaterials [17–19] under the external direct current (DC) magnetic fields, as polarization-independent phenomena – magnetochiral (MCh) and optical magneto-electric (ME) effects [20, 21]. Although such nonreciprocal MCh metamaterials indicate the presence of room-temperature coherent couplings between magnons and photons at microwave frequencies [18], the coupling mechanism remains unclear. The coupling mechanism should be therefore clarified by evaluating the coupling ratios of the MP.

In this Letter, we demonstrate experimentally and numerically ultrastrong couplings of the directionally-nonreciprocal MPs in a single three-dimensional MCh metamolecule at room temperature. The coupling ratio is evaluated to be $g/\omega > 0.2$, which is achieved by direct interaction between magnons in the yttrium-iron garnet (YIG) cylinder and microwave photons in the Cu chiral structure as a resonator. The further enhancement of the coupling ratio can be achieved by a decrease in the frequency of the fundamental mode of the chiral resonance, bringing about the deepstrong-coupling for hybrid quantum systems. Moreover, the metamolecule including the chiral resonator paves a way to the directionally-nonreciprocal MPs in the free-space for synthetic gauge fields for photons. Furthermore, the synthesis of metamolecules and metamaterials by

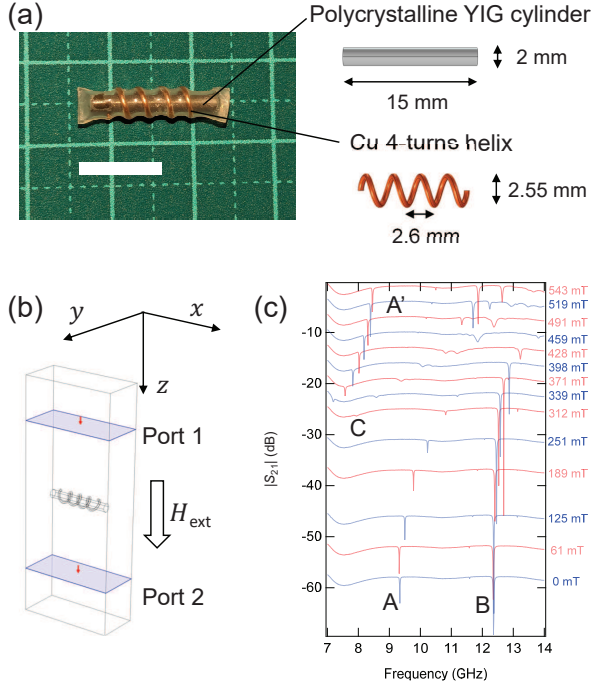


FIG. 1. Magneto-chiral (MCh) metamolecule under study, measurement setup, and measured microwave spectra of the metamolecule. (a) Sample photo and constituents. A white bar corresponding to 10 mm. (b) Measurement and simulation setup of the x -axis-oriented metamolecule placed in a waveguide. (c) $|S_{21}|$ amplitude spectra of the x -axis-oriented metamolecule at various magnetic fields.

combining different meta-atoms leads to quasi-particle “chemistry”.

Experimental setup – Figure 1(a) is an illustration of the MCh metamolecule. The MCh metamolecule consists of a polycrystalline YIG cylinder (as a magnetic meta-atom) inserted in a right-handed helix made of copper (Cu) (as a chiral meta-atom) [18]. The Cu wire of 0.55 mm diameter is wound four times with a 2.6 mm pitch to form the right-handed helix of a 2.55 mm outer diameter. The YIG cylinder is 2 and 15 mm in diameter and length, respectively.

As in Fig. 1(b), the MCh metamolecule is set into a WR-90 waveguide that supports the TE_{10} mode with square flange adapters (Pasternack PE9804). The metamolecule is oriented along the x -axis, which is parallel to the AC magnetic field in the WR-90 waveguide. See Fig. S1 in Supplemental Material [22] for AC magnetic and electric fields of the TE_{10} mode in the waveguide. An external DC magnetic field, $\mu_0 H_{\text{ext}}$, up to approximately 540 mT is applied in the $+z$ direction by an electromagnet. The waveguide is connected to a vector network analyzer (VNA) (Rohde & Schwarz ZVA67) with a microwave input power of 0 dBm (1mW). The S parameters are measured using VNA. The S_{21} indicates a complex transmission coefficient from port 1 to 2, while S_{12} repre-

sents that from port 2 to 1. All measurements are carried out at room temperature.

Experimental results – Figure 1(c) illustrates the transmission amplitude $|S_{21}|$ spectra of the x -axis-oriented MCh metamolecule from 7 to 14 GHz under varying $\mu_0 H_{\text{ext}}$ (0 - 543 mT). Without the DC magnetic field ($\mu_0 H_{\text{ext}} = 0$), two sharp dips are observed: one at 9.34 GHz (A) and the other at 12.36 GHz (B). Based on numerical simulation using COMSOL Multiphysics of the metamolecule under $\mu_0 H_{\text{ext}} = 0$, we confirm that a dip at the lowest frequency is caused by the third-order resonance, with two nodes in the Cu chiral meta-atom induced by the microwave photons with the AC magnetic field in the x -axis (See Fig. S2(a) and Movie S1 in Supplemental Material [22]). The dip (A) at 9.34 GHz is thus traced back to the resonating photons, referred to as chiral resonant photons, because the chiral meta-atom functions as a resonator or sensitizer. Contrastingly, the dip (B) at the higher frequency is not caused by simple resonance but by a complex mode with tornado-like current distribution in the Cu chiral structure or Mie resonance by the displaced YIG cylinder (Figs. S2(a) and S2(c) and Movie S2 in Supplemental Material [22]). Therefore, in this experiment, we focus on the third-order chiral resonant photon at approximately 9 GHz, which is labeled as (A).

Applying the external DC magnetic field to the metamolecule in the $+z$ -direction causes the chiral resonant photon mode (A) to shift slightly to a lower frequency at $\mu_0 H_{\text{ext}} = 61$ mT and then turn to a higher frequency with increasing $\mu_0 H_{\text{ext}}$. The major blue shift of the chiral resonant photon mode is attributed to the magnetic permeability change of the YIG cylinder by the applied $\mu_0 H_{\text{ext}}$, which is the evidence of the interaction between the YIG magnetic meta-atom and the microwave photon in the Cu chiral meta-atom. When $\mu_0 H_{\text{ext}} = 312$ mT, a slight dip appears at approximately 8 GHz labeled as (C) in Fig. 1(c). The slight dip keeps moving to a higher frequency with an increase in $\mu_0 H_{\text{ext}}$ up to 543 mT; therefore, the dip is caused by ferromagnetic resonance, i.e., a magnon, in the YIG magnetic meta-atom. When $\mu_0 H_{\text{ext}} = 339$ mT, the magnon mode (C) approaches the chiral resonant photon mode (A). Simultaneously, another sharp dip appears at 7.19 GHz, denoted by (A'), and shifts to a higher frequency with a further increase in $\mu_0 H_{\text{ext}}$. This indicates the hybridization of chiral resonant photon modes (A) and (A') with the magnon mode (C), demonstrating the coherent coupling between chiral resonant photons and magnons in the metamolecule.

In Fig. 2(a), $|S_{21}|$ is plotted two-dimensionally as functions of $\mu_0 H_{\text{ext}}$ of 0 - 543 mT (horizontal axis) and of frequency of 7 - 14 GHz (vertical axis) to evaluate magnon-photon coupling strength. The black color corresponds to a higher transmission in the $|S_{21}|$ spectra, while the yellow to white colors correspond to lower transmissions. Green dotted lines correspond to eye guides of the chiral

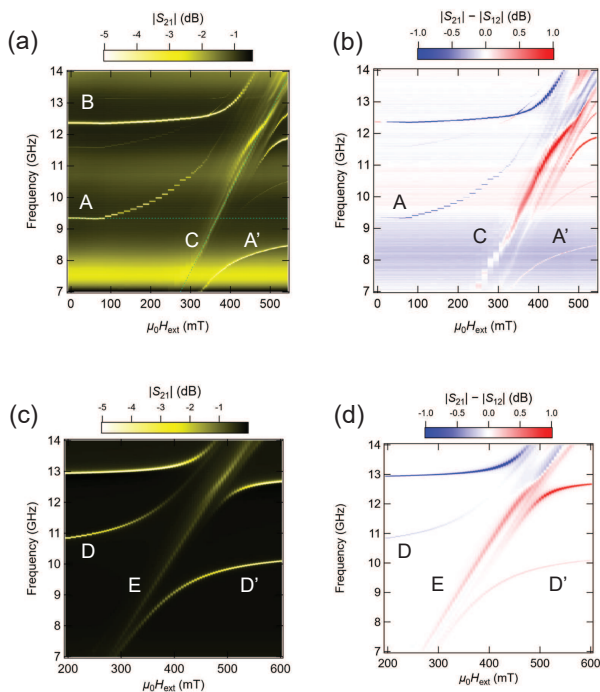


FIG. 2. Two dimensional plot of measured and simulated MP's dispersions. Measured 2D plots of (a) transmission amplitude $|S_{21}|$ and (b) amplitude difference $|S_{21}| - |S_{12}|$ of x -axis-oriented metamolecule as functions of applied external DC magnetic field, $\mu_0 H_{\text{ext}}$, and frequency. (c) and (d) are 2D plots numerically simulated using COMSOL Multiphysics, corresponding to (a) and (b), respectively.

resonant photon frequency and the magnon dispersion. The $|S_{21}|$ two-dimensional (2D) plot in Fig. 2(a) highlights, at $\mu_0 H_{\text{ext}} \sim 350$ mT, the anti-crossing between the chiral resonant photon mode (A) with $\omega_a/2\pi = 9.34$ GHz and magnon mode (C). The anti-crossing Rabi-like level splitting of chiral resonant photon modes (A) and (A') is $g/\pi = 4.19$ GHz at $\mu_0 H_{\text{ext}} = 367.7$ mT, resulting in a coupling ratio of $g/\omega_a = 0.22$. Figure 2(a) demonstrates that magnons in the YIG cylinder and photons in the Cu chiral structure in the MCh metamolecule are ultra-strongly coupled at room temperature. The coupling ratio can be varied by the metamolecule orientation. Figures S3(a), S3(b), and S3(c) in Supplemental Material [22] indicate that the z -axis-orientated metamolecule has a smaller coupling. The coupling ratio is thus relevant to the electromagnetic mode.

Figures S4(a) and S4(b) in Supplemental Material [22] present the directional transmission amplitude difference, $|S_{21}| - |S_{12}|$, and phase difference, $\arg S_{21} - \arg S_{12}$, spectra of the MCh metamolecule in the x -axis orientation, respectively. Using Fig. S4(a), a 2D plot of experimentally observed $|S_{21}| - |S_{12}|$ is drawn in Fig. 2(b). The red color corresponds to $|S_{21}| > |S_{12}|$, while the blue color corresponds to $|S_{21}| < |S_{12}|$. The chiral resonant photon mode (A) above the magnon mode line (C) demonstrates

$|S_{21}| < |S_{12}|$, while the mode (A') below the magnon mode (C) represents $|S_{21}| > |S_{12}|$. This is characteristic of the directional nonreciprocity of ultrastrongly-coupled MP.

Numerical simulation – Simultaneous breaking of time-reversal and space-inversion symmetries by the co-existence of magnetism and chirality in the metamolecule is the primary origin of the directional nonreciprocity observed in Fig. 2(b). An alternative and artificial origin could be a slight displacement of the metamolecule from the waveguide center or a misalignment of the metamolecule from the x -axis because similar nonreciprocal signals have been observed by an asymmetrical microstrip line on a ferrite substrate [23] and a displaced magnetic material on a coplanar waveguide [24]. Indeed in this study, numerical simulation indicates that the dip (B) observed at a higher frequency is caused by the Mie resonance of the displaced YIG cylinder (Figs. S2(a) and S2(c) in Supplemental Material [22]). Therefore, we conduct numerical simulations of the metamolecule under various magnetic fields using COMSOL Multiphysics to exclude such an artificial origin. The Supplemental Material [22] details the numerical simulation method (see also reference [25] therein).

Figure 2(c) presents a numerically simulated 2D plot of $|S_{21}|$ as functions of $\mu_0 H_{\text{ext}}$ of 200 - 600 mT (horizontal axis) and of 7 - 14 GHz frequency (vertical axis). Level repulsion due to the interaction between chiral resonant photons (D and D') and magnons (E) is reproduced. The simulated coupling ratio of 0.15 derived from the level splitting of 3.21 GHz at $\mu_0 H_{\text{ext}} = 410$ mT is smaller than that observed experimentally in Fig. 2(a) because the magnetization dynamics in the YIG cylinder is linearized in the numerical simulation. Nevertheless, the simulated 2D plot of $|S_{21}| - |S_{12}|$ in Fig. 2(d) has successfully reproduced the directional nonreciprocity of the MPs. The metamolecule has negligible dissipation and is regarded as a Hermitian system. As shown in Fig. 2(d), removal of the misalignment and displacement of the metamolecule in the simulation verifies that the origin of directionally-nonreciprocal signals is the MP under the simultaneous breaking of time-reversal and space-inversion symmetries in the metamolecule.

Theoretical consideration – The coupling ratio of the MP is quantitatively reproduced by considering the magnetization dynamics. The experimental system is the forced oscillation of MPs driven by the input microwaves; nonetheless, a simpler damped oscillation model is assumed to evaluate the coupling ratio of the magnon and chiral resonant photons in the following. As in Fig. 3(a), $h_{n,x}$ represents an AC magnetic field in the x -direction due to the Ampère's circuital law accompanied by the Faraday's electromagnetic induction in the chiral meta-atom – chiral resonant photons. Here, the integer n denotes the mode-index of the chiral resonant photons. The AC magnetic field $h_{n,x}$ excites magnons (m_x) in the YIG

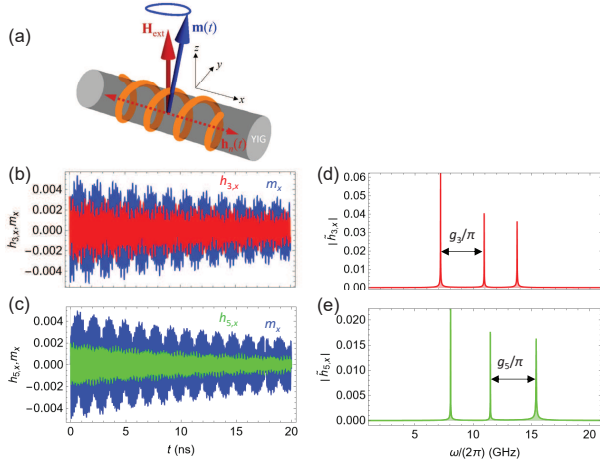


FIG. 3. Theoretical consideration including magnetization dynamics. (a) Schematic of MCh metamolecule composed of a Cu chiral structure involving a YIG cylinder. The metamolecule's YIG cylinder is oriented to the x -axis. (b) and (c) Rabi-like oscillations of the chiral resonant photons ($h_{n,x}$) and magnon (m_x) under $\mu_0 H_{\text{ext}} = 0.39$ T ($n = 3$) and $\mu_0 H_{\text{ext}} = 0.50$ T ($n = 5$), respectively. (d) and (e) Corresponding Fourier spectra of chiral resonant photons ($h_{n,x}$) for 9.34 GHz and 12.36 GHz, respectively.

cylinder. This leads to direct coupling between magnons and chiral resonant photons, generating ultrastrongly-coupled MPs in the metamolecule. Recall that the numerical simulation using COMSOL indicates that the third-order resonance with $n = 3$ ($h_{3,x}$) appears at approximately 10 GHz. Thus, the MPs can be described as a coupled oscillator model that considers a uniform magnon mode and two chiral resonant modes with $n = 3$ and 5. The Supplemental Material [22] presents the calculation details (see also reference [26] therein).

Figures 3(b) and 3(c) are calculated damped oscillations of the chiral resonant photons ($h_{n,x}$) and the magnons (m_x) under $\mu_0 H_{\text{ext}} = 0.39$ T for $n = 3$ and under $\mu_0 H_{\text{ext}} = 0.50$ T for $n = 5$, respectively. We assume the higher frequency mode to be the fifth-order resonance. The time evolutions in Figs. 3(b) and 3(c) correspond to Rabi-like oscillations – the amplitude exchange between one chiral resonant photon (red or green) and a magnon (blue). A minimal complexity in the Rabi-like oscillations is attributed to interactions among three modes (one magnon and two chiral resonant photons) in the metamolecule.

Figures 3(d) and 3(e) correspond to the Fourier spectra of the time evolutions, in which three peaks represent coupled modes among one magnon and two chiral resonant photons, i.e., MP modes with the Rabi-like frequency splitting. According to these spectra, the evaluated couplings are $g_3/\pi = 3.75$ GHz and $g_5/\pi = 3.93$ GHz, resulting in the coupling ratios of $g_3/\omega_3 = 0.20$ and $g_5/\omega_5 = 0.16$, respectively. Here, the subscripts in

g_n and ω_n mean the corresponding values of the n -th order. Based on the experimental results, $\omega_3/2\pi = 9.34$ and $\omega_5/2\pi = 12.36$ GHz are assumed for this evaluation. The computed $g_3/\omega_3 = 0.20$ is consistent with the experimentally obtained $g/\omega_a = 0.22$, indicating that MP in the MCh metamolecule is in the ultrastrong coupling regime. Moreover, $g_3/\omega_3 = 0.20$ and $g_5/\omega_5 = 0.16$ indicate that the coupling at a lower frequency is much stronger than that at a higher frequency.

Discussion – This study reveals that the MCh metamolecule consisting of a YIG cylinder inserted in a Cu chiral structure results in ultrastrongly-coupled and directionally-nonreciprocal MP at room temperature. Table S1 in Supplemental Material [22] compares the temperature, MP coupling ratio, and nonreciprocity obtained in this study with those reported in the literature (see also references [27, 28] therein). Ultrastrong coupling in the MP is primarily caused by direct interaction between photons in the Cu chiral structure and magnons in the magnetic YIG cylinder via AC magnetic fields in the x -direction. The coupling ratio is reduced in the z -axis-orientated metamolecule (Fig. S3(c)) because electromagnetically induced AC magnetic fields in the z -direction cannot drive magnons under the external DC magnetic field, $\mu_0 H_{\text{ext}}$, in the z -direction. This results in indirect coupling between the chiral resonant photon and magnon in the z -axis-orientated metamolecule. Therefore, the coupling ratio can be enhanced by finding a suitable metamolecule orientation.

Utilizing the fundamental mode ($n = 1$) is another strategy toward achieving a much stronger coupling between magnons and photons – the deepstrongly-coupled MP, i.e., $g/\omega_a \geq 1$, in the metamolecule. This experiment uses the third-order mode ($n = 3$) of the chiral resonant photon to obtain the highest value of $g/\omega_a = 0.22$; the magnon-photon coupling is thus reduced by $\eta_3 = 1/3$, where η_n is a phenomenologically introduced mode-dependent coefficient responsible for the space-dependence of the microwave magnetic field in the MCh metamolecule. Here, we assume the net magnitude of the AC magnetic field of the chiral resonant photon to be inversely proportional to the number of antinodes (See more detailed in Supplemental Material [22]). In this way, the $n = 1$ fundamental mode may enhance the magnon-photon coupling by maximizing the electromagnetic induction due to the magnon dynamics.

Additionally, according to the theoretical prediction for the metamolecule [29], the coupling ratio is evaluated via $g/\omega_a \propto 1/\sqrt{\omega_a}$. Therefore, further enhancement toward the deepstrong-coupling is possible by decreasing the chiral resonant frequency, ω_a , of the fundamental mode by increasing the system size and changing the design of the metamolecule and materials of the constitutive meta-atoms. The deepstrongly-coupled MP will lead to mysterious quantum effects, such as the vacuum Bloch-Siegert shift [30] and quantum squeezing under thermal

equilibrium [31]. The Hermitian, ultrastrongly-coupled, and directionally-nonreciprocal MP may give rise to coherent quantum rectification of quantum information.

The second origin of the ultrastrong coupling in this study is the photon confinement in the chiral meta-atom. The chiral meta-atom functions as a resonator or sensitizer; because the resonator is embedded in the metamolecule that supports MPs, the MPs for propagating microwaves in the free-space can be realized using the metamolecule. As shown in Fig. S5 in Supplemental Material [22], our additional numerical simulation using COMSOL verifies the free-space MP with ultrastrong coupling and directional nonreciprocity. The MP in the free-space is a central topic in quantum optics as it allows control over individual quantum systems [32, 33]. Moreover, the nonreciprocal MP in the free-space leads to the observation of the polarization-independent optically-moving effects. The optically-moving effect in the MCh and ME media exhibits an electromagnetic response equivalent to that of a regular material moving at a relativistic speed [34–36]. Therefore, free-space MPs with ultrastrong coupling and directional nonreciprocity enable us to realize synthetic gauge fields, i.e., the Lorentz force acting on the propagating microwaves [37].

Last but not least, the quasi-particle integration is comprehensively classified according to the interaction between polarization P and magnetization M . The conventional ME and MCh effects observed in this study are given by the coupling between P and M . Contrastingly, the dynamic coupling of time-derivatives of P and M results in a new collective mode corresponding to an MCh electromagnon-polariton, which is still unclear but anticipated to be observed using metamaterials. Furthermore, we focus on magnons in this study; however, other quasi-particles, such as, excitons, phonons, and plasmons, can be integrated in the metamaterials. Thus, this study signifies a pivotal advancement toward expounding quasi-particle “chemistry” using metamaterials.

Conclusion – We demonstrate ultrastrong couplings of the directionally-nonreciprocal MPs in a single three-dimensional MCh metamolecule at room temperature. The metamolecule exhibits the coupling ratio of $g/\omega = 0.22$, which is achieved by direct interaction between magnons in the YIG meta-atom and microwave photons confined in the Cu chiral meta-atom as the resonator. These experimental results are reproduced well via numerical simulations and theoretical consideration. The coupling ratio and directional nonreciprocity can be enhanced by changing the metamolecule orientation and the chiral resonance frequency. The MCh metamolecule represents a crucial step toward developing the hybrid quantum systems and quasi-particle “chemistry” using metamaterials. Furthermore, the optically-moving MPs by the metamolecules in the free-space enable us to realize the Lorentz force acting on the propagating mi-

crowaves.

Acknowledgements – We thank H. Yasuda and Y. Motoda for their technical support with the microwave measurements and H. Kurosawa for helping with the numerical simulation. This work is financially supported by JSPS-KAKENHI (JP24H02232, 23K13621, 22K14591) and JST- CREST (JPMJCR2102).

* Email address:tomita@tohoku.ac.jp

- [1] A. F. Kockum, A. Miranowicz, S. De Liberato, S. Savasta, and F. Nori, *Nat. Rev. Phys.* 1, 19 (2019).
- [2] P. Forn-Diaz, L. Lamata, E. Rico, J. Kono, and E. Solano, *Rev. of Mod. Phys.* 91, 025005 (2019).
- [3] Y. Li, W. Zhang, V. Tyberkevych, W.-K. Kwok, A. Hoffmann, and V. Novosad, *J. Appl. Phys.* 128, 130902 (2020).
- [4] M. Harder, B. M. Yao, Y. S. Gui, and C.-M. Hu, *J. Appl. Phys.* 129, 201101 (2021).
- [5] D. Lachance-Quirion, Y. Tabuchi, A. Gloppe, K. Usami, and Y. Nakamura, *Appl. Phys. Exp.* 12, 070101 (2019).
- [6] G. Bourcin, J. Bourhill, V. Vlaminck, and V. Castel, *Phys. Rev. B* 107, 214423 (2023).
- [7] I. Golovchanskiy, N. N. Abramov, V. S. Stolyarov, A. A. Golubov, M. Yu. Kupriyanov, V. V. Ryazanov, and A. V. Ustinov, *Phys. Rev. Appl.* 16, 034029 (2021).
- [8] I. A. Golovchanskiy, N. N. Abramov, V. S. Stolyarov, M. Weides, V. V. Ryazanov, A. A. Golubov, A. V. Ustinov, and M. Y. Kupriyanov, *Sci. Adv.* 7, eabe8638 (2021).
- [9] A. Ghirri, C. Bonizzoni, M. Maksutoglu, A. Mercurio, O. Di Stefano, S. Savasta, and M. Affronte, *Phys. Rev. Appl.* 20, 024039 (2023).
- [10] M. Harder and C.-M. Hu, *Solid State Phys.* 69, 47 (2018).
- [11] M. Harder, Y. Yang, B. M. Yao, C. H. Yu, J. W. Rao, Y. S. Gui, R. L. Stamps, and C. M. Hu, *Phys. Rev. Lett.* 121, 137203 (2018).
- [12] X. Zhang, A. Galda, X. Han, D. Jin, and V. M. Vinokur, *Phys. Rev. Appl.* 13, 044039 (2020).
- [13] L. D. Barron, J. Vrbancich, *Mol. Phys.* 51, 715 (1984).
- [14] G. L. J. A. Rikken and E. Raupach, *Nature* 390, 493 (1997).
- [15] M. Vallet, R. Ghosh, A. Le Floch, T. Ruchon, F. Bretenaker, and J.-Y. Thépot, *Phys. Rev. Lett.* 87, 183003 (2001).
- [16] Y. Okamura, F. Kagawa, S. Seki, M. Kubota, M. Kawasaki, and Y. Tokura, *Phys. Rev. Lett.* 114, 197202 (2015).
- [17] S. Tomita, K. Sawada, A. Porokhnyuk, and T. Ueda, *Phys. Rev. Lett.* 113, 235501 (2014).
- [18] S. Tomita, H. Kurosawa, K. Sawada, and T. Ueda, *Phys. Rev. B* 95, 085402 (2017).
- [19] S. Tomita, H. Kurosawa, T. Ueda, and K. Sawada, *J. Phys. D: Appl. Phys.* 51, 083001 (2018).
- [20] Y. Tokura and N. Nagaosa, *Nat. Commun.* 9, 3740 (2018).
- [21] S. Toyoda, N. Abe, and T. Arima, *Phys. Rev. Lett.* 123, 077401 (2019).
- [22] See Supplemental Material at URL.
- [23] T. Ueda and M. Tsutsumi, *IEICE Trans. Electron.* E89-C, 1318–23 (2006).

- [24] T. Kodama, Y. Kusanagi, S. Okamoto, N. Kikuchi, O. Kitakami, S. Tomita, N. Hosoito, and H. Yanagi, *Phys. Rev. Appl.* 9, 054025 (2018).
- [25] D. M. Pozar, *Microwave Engineering 3rd. Edition* (John Wiley & Sons, 2005).
- [26] Y. Cao, L. He, and P. Zhuang, *Phys. Rev. D* 91, 094423 (2015).
- [27] X. Zhang and M. Sarovar, *Phys. Rev. Lett.* 113, 156401 (2014).
- [28] L. Bai, M. Harder, Y. P. Chen, X. Fan, J. Q. Xiao, and C.-M. Hu, *Phys. Rev. Lett.* 114, 227201 (2015).
- [29] T. Chiba, T. Komine, and T. Aono, *J. Mag. Soc. Jpn.* 48, 21 (2024).
- [30] X. Li, M. Bamba, Q. Zhang, S. Fallahi, G. C. Gardner, W. Gao, M. Lou, K. Yoshioka, M. J. Manfra, and J. Kono, *Nat. Photo.* 12,324 (2018).
- [31] K. Hayashida, T. Makihara, N. Marquez Peraca, D. Fallas Padilla, H. Pu, and J. Kono, M. Bamba, *Sci. Repo.* 13, 2526 (2023).
- [32] A. Bayer, M. Pozimski, S. Schambeck, D. Schuh, R. Huber, D. Bougeard, and C. Lange, *Nano Lett.* 17, 6340–6344 (2017).
- [33] S. Rajabali, S. Markmann, E. Jöchl, M. Beck, C. A. Lehner, W. Wegscheider, J. Faist, and G. Scalari, *Nat. Commun.* 13, 2528 (2022).
- [34] J. A. Kong, *Electromagnetic Wave Theory* (EMW Publishing, Cambridge, 2005).
- [35] V. S. Asadchy, A. Díaz-Rubio, and S. A. Tretyakov, *Nanophotonics* 7, 1069 (2018).
- [36] T. Kodama, T. Nakanishi, K. Sawada, S. Tomita, *Opt. Mater. Exp.* 14, 2499 (2024).
- [37] K. Sawada and N. Nagaosa, *Phys. Rev. Lett.* 95, 237402 (2005).